

Backstepping approach for the control of the double-fed asynchronous generator in a wind power system

Mbarek Chahboun¹, Mohcine Abouyaakoub¹, Ali Ait Ali¹, Aziz El Mrabet¹,
Hicham Hihhi¹, Hassan Ouabi², Youssef El Bid³

¹Laboratory of Engineering Systems and Applications, Nationale School of Applied Sciences, Sidi Mohamed Ben Abdellah University, Fez, Morocco

²Department of Electrical Engineering, Higher Normal School of Technical Education Mohammedia, Hassan II University, Casablanca, Morocco

³Energies and Sustainable Development Research Team, Higher School of Technology, Ibn Zohr University, Agadir, Morocco

Article Info

Article history:

Received Mar 24, 2024

Revised Sep 7, 2024

Accepted Sep 29, 2024

Keywords:

Backstepping
Control system

DFIG

Fuzzy logic

Renewable energy

Wind turbine

ABSTRACT

This paper aims to model and control the dual-fed asynchronous generator (DFIG). The modeling and vector control were simulated using MATLAB, followed by the application of the Backstepping control strategy. A comparative study between two DFIG control strategies, fuzzy logic control (FLC) and Backstepping control, was conducted. The results for the Backstepping approach are discussed and compared with FLC, highlighting that the Backstepping technique addresses robustness issues regarding variations in operating conditions and internal parameters. Both control strategies are applied to a wind turbine system, and the simulation results and robustness tests are analyzed.

This is an open access article under the [CC BY-SA](https://creativecommons.org/licenses/by-sa/4.0/) license.



Corresponding Author:

Mbarek Chahboun

Laboratory of Engineering, Systems and Applications, Nationale School of Applied Sciences

Sidi Mohamed Ben Abdellah University

Fez, Morocco

Email: mbarek.chahboun@usmba.ac.ma

1. INTRODUCTION

Wind power, with its capacity to meet global energy needs and reduce greenhouse gas emissions, is vital for the transition to sustainable energy sources. Efficient regulation of double-fed induction generators (DFIGs) is key to optimizing wind energy output and maintaining grid stability. A literature review highlights significant contributions in this field. Various control methods for DFIGs, such as the Backstepping approach and fuzzy logic control (FLC), have been examined. Studies [1]-[5] have shown the benefits of the Backstepping approach in enhancing system performance and stability. Other research [6]-[10] has demonstrated the adaptability and flexibility of fuzzy logic in controlling DFIGs in wind farms. However, previous studies have not explicitly compared the influence of Backstepping and fuzzy logic on specific performance metrics under varying operating conditions. To address these gaps, our research analyzes the use of the Backstepping approach and fuzzy logic for controlling DFIGs in wind power systems. By comparing these methods and evaluating their performance, we aim to identify weaknesses in existing literature and suggest improvements. Our research integrates advanced control methods to push the field of wind energy forward. We provide an in-depth analysis of the Backstepping and fuzzy logic approaches to DFIG control, aiming to inform the design and implementation of future wind energy systems for a more sustainable and efficient energy transition. This paper presents a detailed Backstepping-based control approach for DFIGs used in wind power systems. Previ-

ous work by Ladide *et al.* [11], Hihi and Rahmani [12], and Soulouh *et al.* [13] has enabled us to design an innovative control method that improves DFIG performance while ensuring stability. Additionally, we conduct a detailed analysis of the Backstepping approach and FLC, highlighting the advantages and disadvantages of each method. Extensive simulations, building on research by Moumani *et al.* [14] and Nadour *et al.* [15], confirm the effectiveness of our control method.

Finally, we discuss the practical implications of our results and their potential impact on further developing wind energy systems. Our method aims to advance ongoing research by offering practical and innovative solutions for controlling DFIGs in current wind power systems. The following sections will detail our research approach, results, and conclusions, emphasizing the relevance and importance of our work in wind system control.

2. METHOD

This section outlines the methodology for modeling and controlling a DFIG in a wind energy system. While previous studies have explored these systems, they have not sufficiently addressed the robustness of control strategies given their inherent non-linearity. We sequentially model the wind turbine, the dual-supply asynchronous generator, and the simulation, including technical details, parameters, and simulation schemes (Jones *et al.* [1], Smith *et al.* [2]). Due to its effectiveness in complex dynamic system modeling, MATLAB/Simulink was utilized. We found that the nonlinear Backstepping controller effectively regulates reactive and active powers. FLC demonstrated flexibility in adapting to operational and environmental changes Wang *et al.* [8]. Our results correlate with Chen *et al.* [7], who highlighted the comprehensive nature of generator control algorithms, focusing on the underlying theoretical principles. Parametric changes on mutual inductance L_m and rotor resistance R_r were conducted to evaluate control system stability, validating our simulation results (Huang). Despite these findings, further in-depth studies are needed to confirm our approach, especially regarding parametric variations. We recommend consulting supplementary references for a thorough confirmation. Our study demonstrates that both Backstepping and fuzzy control methods are robust, with the system exposed to active and reactive power levels to monitor regulator behavior. Future research should explore these methods in more diverse operational scenarios to enhance the reliability of control strategies.

3. MODELLING THE WIND ENERGY SYSTEM

The wind energy system is made up of various crucial parts that make sure it works. These consist of a machine-side converter, a doubly-fed asynchronous generator (DFIG), a gearbox, and a turbine. The energy conversion process starts when wind energy is captured by the turbine and then sent to the DFIG to be converted into electrical energy. A wind turbine with three blades of length R that are powered by a generator is employed in the system under study. A gain multiplier G is included in this arrangement to increase the generated power.

3.1. Wind modelling

The initial phase of establishing a wind power project involves meticulously choosing the site's geographic location. It is necessary to closely examine the wind characteristics since the power produced by a wind energy system is directly related to the cube of the wind speed. To gain an in-depth understanding of the particularities of a given site, it is essential to collect data on wind direction and speed over an extended period [4]. In our study, we used a specific wind model [5] whose expression is in (1).

$$v(t) = 8 + 0.2 * \sin(0.1047.t) + 0.2 * \sin(3.6645.t) + 2.\sin(0.2665.t) \quad (1)$$

This mathematical model enabled us to analyse in greater detail the fluctuations in wind speed over time at the site studied, for a detailed description of this part, please refer to our previous article [16].

3.2. Turbine modelling

The part of the system responsible for converting wind energy from kinetic to mechanical is the wind turbine. When wind hits the turbine blades at a particular speed v , it generates mechanical energy on the turbine shaft, making the blades spin. The aerodynamic power harnessed by the turbine rotor is expressed by (1).

$$P_t = \frac{1}{2} . C_p(\lambda, \beta) . \rho . S . v^3 \quad (2)$$

Typically, the power coefficient is shown as a function of the tip speed ratio λ in relation to the angle β , which is the angle formed between the rotation direction and the chord line of the blade section. The tip speed ratio of a wind turbine is explained as (3):

$$\lambda = \frac{u}{v} = \frac{\Omega_t \cdot R}{v} \quad (3)$$

where: ρ : the density of the air, λ : relative speed is the ratio of wind speed to linear speed at the turbine blade tips, Ω_t : the turbine's rotational speed, R : the blade's length, S : the circle that the turbine sweeps, v : the wind speed and C_p : the coefficient of power, for a detailed description of this part, please refer to our previous article [16].

4. DFIG MODELLING

There is a plethora of research on the modeling of the doubly-fed induction generator (DFIG) in the literature [1]-[3]. The mathematical model of the DFIG is quite simple in design, but it is remarkably sophisticated. Its nonlinear and multivariable structure and the interplay of electrical, magnetic, and mechanical events during operation [17] are the causes of this complexity. One feature of the DFIG model is that it generates differential equations whose coefficients change over time in response to the rotor's position inside a fixed three-phase reference frame that is linked to the stator. This raises the machine's modeling complexity even more [4]. For a detailed description of this part, please refer to our previous article [18].

4.1. Vector control of DFIG

By manipulating the rotor flux of the DFIG, it becomes possible to regulate both active and reactive power. This approach guarantees that the armature reaction flux and rotor flux maintain a perpendicular relationship. To autonomously regulate the stator power [19], it becomes essential to independently control the transverse voltages of the rotor and armature by introducing compensation terms, thus attaining a decoupled control mode [20]. By making adjustments from (23) to (18), the rotor voltages can be redefined. The following Figure 1 shows the regulated system's block diagram. For a detailed description of this part, please refer to our previous article [21].

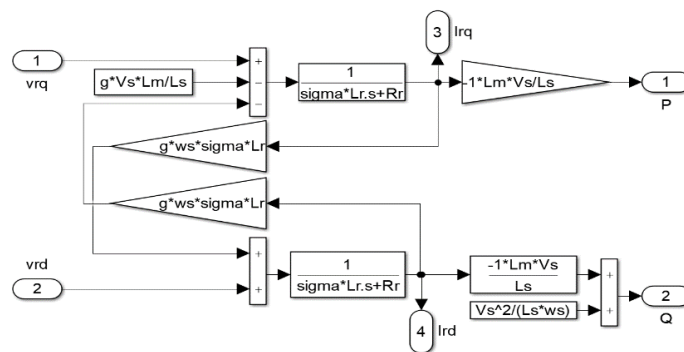


Figure 1. Block schematic of the regulated system

5. THE PRINCIPLE OF THE BACKSTEPPING COMMAND

The fundamental principle of Backstepping control is to reorganise closed-loop systems into subsets of lower-order subsystems, each of which is stabilised according to the Lyapunov criterion. This approach gives these systems robustness properties and ensures their overall asymptotic stability. In other words, it is a multi-stage process in which, at each stage [22], a virtual control is generated to ensure that the system converges towards the desired equilibrium state. This convergence is achieved progressively through the use of Lyapunov functions that ensure step-by-step stabilisation.

5.1. The control of non-linear systems is based on two Lyapunov approaches

Lyapunov's first method assesses a system's stability by linearizing its dynamics around an equilibrium point, focusing on local stability. While useful for understanding stability near the equilibrium, it does

not address the system's overall stability and overlooks nonlinear phenomena. This method helps determine if a broader stability analysis is needed.

The second Lyapunov method, on the other hand, evaluates stability based on energy considerations without solving the nonlinear differential equations of the system. Stability is judged by how an energy function changes as the system evolves. To assess stability, one seeks a positive definite function $V(x)$ that represents the system's energy, with its derivative being negative semi-definite in the relevant region. Backstepping control provides a framework for designing control strategies for complex dynamic systems, ensuring their stability and convergence to desired equilibrium states [23].

5.1.1. Active power control

First, let's examine active power control. The following is the definition of the active power tracking,

$$e_1 = P_s^* - P_s \quad (4)$$

take a look at this potential Lyapunov function,

$$V(e_1) = \frac{1}{2} \cdot e_1^2 \quad (5)$$

the Lyapunov candidate function's derivative,

$$\dot{V}(e_1) = e_1 \cdot \dot{e}_1 \quad (6)$$

$$\dot{e}_1 = \dot{P}_s^* - \dot{P}_s = \dot{P}_s^* + \left(1 - \frac{M_{sr}^2}{L_s \cdot L_r}\right) \cdot \frac{L_r \cdot L_s}{v_s \cdot M_{sr}} \frac{di_{rq}}{dt} \quad (7)$$

and,

$$\dot{P}_s = \left(\frac{M_{sr}^2}{L_s \cdot L_r}\right) \cdot \frac{L_r \cdot L_s}{v_s \cdot M_{sr}} \frac{di_{rq}}{dt} - 1 \quad (8)$$

The derivative of the current, i_{rq} , can be obtained by substituting the expression into the voltage equation, v_{rq} (28) and getting:

$$\dot{e}_1 = \dot{P}_s^* + \frac{v_s \cdot M_{sr}}{(L_s \cdot L_r - M_{sr}^2)} \left(v_{rq} - R_r \cdot i_{rq} - \left(1 - \frac{M_{sr}^2}{L_s \cdot L_r}\right) \cdot L_r \cdot \omega_r \cdot i_{rd} + g \cdot \frac{v_s \cdot M}{\omega_s \cdot L_s} \right) \quad (9)$$

replacing the last in (7) gives,

$$\dot{V}(e_1) = e_1 \cdot \dot{e}_1 = e_1 \cdot \left(\dot{P}_s^* + \frac{v_s \cdot M_{sr}}{(L_s \cdot L_r - M_{sr}^2)} \left(v_{rq} - R_r \cdot i_{rq} - \left(1 - \frac{M_{sr}^2}{L_s \cdot L_r}\right) \cdot L_r \cdot \omega_r \cdot i_{rd} + g \cdot \frac{v_s \cdot M}{\omega_s \cdot L_s} \right) \right) \quad (10)$$

the following is how we arrive at the stabilizing Backstepping command expression,

$$v_{rq} = -\frac{(L_s \cdot L_r - M_{sr}^2)}{v_s \cdot M_{sr}} \cdot \dot{P}_s^* + R_r \cdot i_{rd} + \omega_r \cdot \left(1 - \frac{M_{sr}^2}{L_s \cdot L_r}\right) \cdot L_r \cdot i_{rd} - g \cdot \frac{v_s \cdot M}{\omega_s \cdot L_s} - \left(1 - \frac{M_{sr}^2}{L_s \cdot L_r}\right) \cdot \frac{L_s \cdot L_r}{v_s \cdot M_{sr}} \cdot k_1 \cdot e_1 \quad (11)$$

to ensure convergence of the Lyapunov candidate function, replacing, expression (11) in (10) gives:

$$\dot{V}(e_1) = -k_1 \cdot e_1^2 < 0 \quad (12)$$

with k_1 positive constant.

5.1.2. Reactive power control

The discrepancy in reactive power tracking is,

$$e_2 = Q_s^* - Q_s \tag{13}$$

this equation provides the increased Lyapunov function,

$$V(e_1, e_2) = \frac{1}{2} \cdot e_1^2 + \frac{1}{2} \cdot e_2^2 \tag{14}$$

its derivative is given by,

$$\dot{V}(e_1, e_2) = e_1 \cdot \dot{e}_1 + e_2 \cdot \dot{e}_2 = -k_1 \cdot e_1^2 + e_2(\dot{Q}_s^* - \dot{Q}_s) \tag{15}$$

with,

$$\dot{e}_2 = \dot{Q}_s^* - \dot{Q}_s = \dot{Q}_s^* + \left(1 - \frac{M_{sr}^2}{L_s \cdot L_r}\right) \cdot \frac{L_r \cdot L_s}{v_s \cdot M_{sr}} \cdot \frac{di_{rd}}{dt} \tag{16}$$

substituting the formula for the derivative of the current i_{rd} into the voltage V_{rd} (27), we arrive at,

$$\dot{e}_2 = \dot{Q}_s^* + \frac{v_s \cdot M_{sr}}{(L_s \cdot L_r - M_{sr}^2)} \left(v_{rd} - R_r \cdot i_{rd} + \left(1 - \frac{M_{sr}^2}{L_s \cdot L_r}\right) \cdot L_r \cdot \omega_r \cdot i_{rq} \right) \tag{17}$$

by substituting the final expression in (15), we acquire,

$$\dot{V}(e_1, e_2) = -k_1 \cdot e_1^2 + e_2 \left(\dot{Q}_s^* + \frac{v_s \cdot M_{sr}}{(L_s \cdot L_r - M_{sr}^2)} \left(v_{rd} - R_r \cdot i_{rd} + \left(1 - \frac{M_{sr}^2}{L_s \cdot L_r}\right) \cdot L_r \cdot \omega_r \cdot i_{rq} \right) \right) \tag{18}$$

the expression for the stabilising Backstepping command is given by,

$$v_{rd} = -\frac{(L_s \cdot L_r - M_{sr}^2)}{v_s \cdot M_{sr}} \cdot \dot{Q}_s^* + R_r \cdot i_{rd} - \omega_r \cdot \left(1 - \frac{M_{sr}^2}{L_s \cdot L_r}\right) \cdot L_r \cdot i_{rq} - \left(1 - \frac{M_{sr}^2}{L_s \cdot L_r}\right) \cdot \frac{L_s \cdot L_r}{v_s \cdot M_{sr}} \cdot k_2 \cdot e_2 \tag{19}$$

if we replace (19) in (18), we obtain,

$$\dot{V}(e_1, e_2) = -k_1 \cdot e_1^2 - k_2 \cdot e_2^2 < 0 \tag{20}$$

with k_2 positive constant.

Figure 2 illustrates the power regulation block diagram for the dual-fed asynchronous machine, utilizing the Backstepping method applied to the machine-side converter.

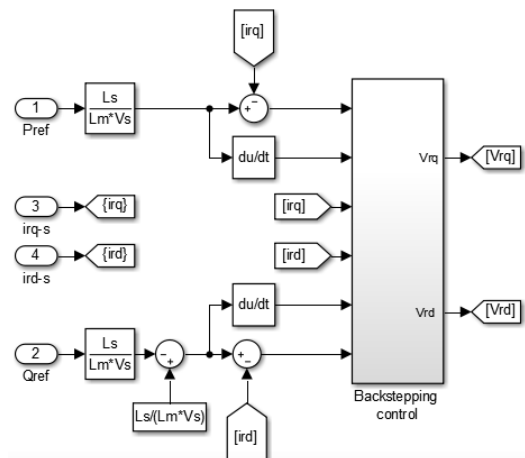


Figure 2. Diagrammatic schematic for DFIM power regulation with the Backstepping technique

5.2. Simulation results

The validation of the DFIG power control method utilizing the Backstepping technique involved rigorous numerical simulations executed via MATLAB/Simulink software. A detailed inventory of the generator parameters is available in the APPENDIXS 1 and 2. To scrutinize the control dynamics and assess its reaction to changes in stator active and reactive power, incremental steps in both active and reactive power were implemented. The ensuing machine response is visually depicted in Figures 3 and 4. Notably, Figure 3 delineates the reactive power response under the Backstepping control scheme employed for the DFIG and Figure 4 illustrates the active power response resulting from the application of Backstepping control to the DFIG.

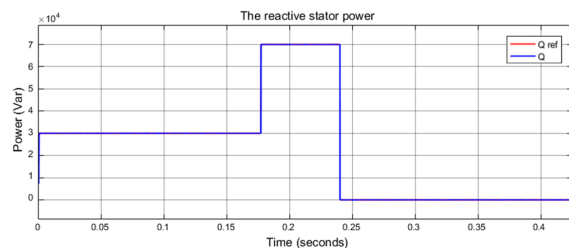


Figure 3. Power response in reaction employing Backstepping control

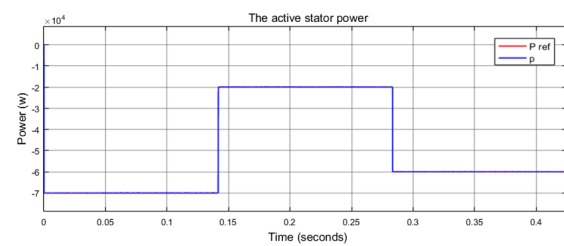


Figure 4. Active power response using Backstepping control

We proceeded to vary the active and reactive power of the system, mirroring previous tests, to assess its regulation capability. Figures 3 and 4 illustrate the simulation outcomes achieved through the Backstepping control method for the doubly-fed asynchronous generator. It's evident that the generator adeptly tracks power variations, whether in active or reactive power. The control depicted in Figures 3 and 4 underscores the satisfactory dynamics of our system. Additionally, virtually zero static error is observed for both active and reactive power. These dynamics respond promptly and exhibit no overshoot. A comparison between the performance of this control and that of an FLC control is outlined in the following paragraph.

6. ACTIVE AND REACTIVE POWER CONTROL BASED ON FUZZY CONTROLLERS

Fuzzy controllers provide a flexible approach for managing both active and reactive power, particularly when creating a mathematical model is difficult or when dealing with nonlinear system behaviors. Their growing use, especially in industrial settings, stems from their ability to handle complex and uncertain systems. Unlike binary logic, fuzzy logic deals with a spectrum of values, capturing the nuances of human reasoning and imprecise language. Introduced by Professor Zadeh, fuzzy logic employs membership functions to handle uncertainty effectively, allowing for efficient control without detailed system modeling.

FLC utilizes linguistic terms and multiple inference rules, enabling operators to apply their expertise and make decisions based on various factors. This discussion will cover the fundamental principles of FLC and the steps involved in implementing it, including the development of an FLC controller for managing the power output of a DFIG.

6.1. Basic fuzzy logic control concepts

The FLC controller operates through four primary phases: the knowledge base, fuzzification, inference engine, and defuzzification. Initially, the controller converts numerical input into fuzzy values. These values are then processed according to fuzzy rules. Finally, the fuzzy values are transformed back into physical values to generate the control signal, as the system operates with physical quantities only [23].

6.2. Fuzzification

In this phase, each variable (current and voltage) is associated with a specific fuzzy subset using quantitative membership functions to describe linguistic variables and quantify their relative uncertainty. Natural language words serve as values for these variables, which act as system inputs or outputs [23]. The inference rules result in an anti-diagonal decision table, summarized in the MACVICAR-WHELAN matrix shown in Table 1, displaying the CF inference matrix for a partition of 7 fuzzy subsets for each input variable e and Δe , for a detailed description of this part, please refer to our previous article [16].

Table 1. The basis of power control rules

| Δe | e | | | | | | |
|------------|-----|----|----|----|----|----|----|
| | NG | NM | NP | ZE | PP | PM | PG |
| NG | TG | TG | TG | G | PG | P | ZE |
| NM | TG | TG | G | G | M | P | TP |
| NP | TG | M | G | TG | TP | P | TP |
| ZE | P | PG | M | ZE | M | PG | P |
| PP | TP | P | TP | TG | G | MG | TG |
| PM | TP | P | M | G | G | TG | TG |
| PG | ZE | P | PG | G | GT | TG | TG |

Where: ZE: zero approximately, TG: very large, P: small, M: average, TP: very positive, PG: large positive, G: large, and the corresponding linguistic values are characterised by symbols such as: NG: very negative, NM: negative average, ZE: zero approximately, NP: small negative, PM: mean positive, and PP: small positive.

6.3. Defuzzification

The core of defuzzification is decision-making, or extracting real control from control obtained as a fuzzy set. While fuzzy rule inference may be used in a variety of ways, the most often used method is the one that determines the membership function's center of gravity. This may be ascertained by applying the generic formula as (21) [24]. Figure 5 presents the schematic design of the FLC for DFIG control.

$$V_R = \frac{\int_{-1}^1 X_k U_R(X_k) dX_k}{\int_{-1}^1 U_R(X_k) dX_k} \quad (21)$$

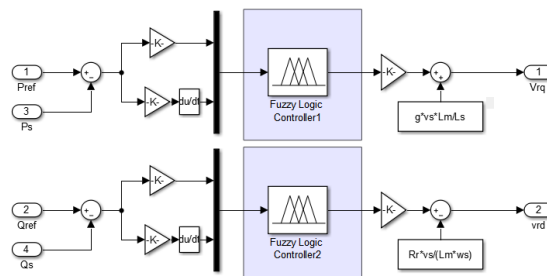


Figure 5. FLC schematic design for DFIG control

6.4. Simulation and results

We therefore subjected the system to changes in active and reactive power (similar to the previous tests) in order to study the behaviour of its regulation. Figures 6 and 7 show the simulation results obtained using DFIG fuzzy control. Figure 6 displays the active power response to FLC control of the DFIG [25], [26], and Figure 7 illustrates the reactive power response resulting from the application of FLC control to the DFIG.

The simulation results show that our system provides better tracking of the power reference, is dynamically satisfactory and the static error tends towards zero with low overshoot (no overshoot for active power). This technique made it possible to achieve perfect decoupling between the two stator power components. In order to better demonstrate the effectiveness of this control, we are going to test the behaviour of the DFIG with the variation of the parameters of the model used.

Robustness tests: parameter identification in machines is prone to inaccuracies due to the methods and measurement devices used. Consequently, the obtained values are often imprecise and subject to variations from factors such as machine heating, load changes, magnetic saturation, air gap shape, and film effects. In this section, we will examine the DFIG's response to changes in model parameters [27]. This will help us understand how parameter variations [28], influenced by operational conditions or identification errors, affect the DFIG's performance.

This analysis is crucial for evaluating the robustness of the control system against such uncertainties and parameter changes. We will test the robustness of both Backstepping and FLCs under simulated conditions to assess their effectiveness [29], [30].

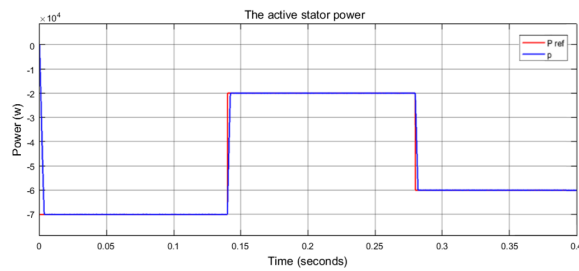


Figure 6. Stator active power response using FLC control

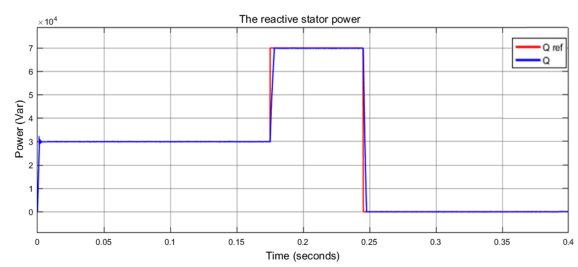


Figure 7. Stator reactive power response using FLC control

6.4.1. Test 1: influence of a +90% variation in rotor resistance R_r

Figure 8 illustrates the impact of variations in rotor resistance on reactive power under Backstepping control of the DFIG and Figure 9 demonstrates how changes in rotor resistance affect active power when employing Backstepping control for the DFIG. Figure 10 illustrates how changes in rotor resistance impact reactive power when utilizing FLC for the DFIG, and Figure 11 illustrates how variations in rotor resistance influence active power when employing FLC for the DFIG.

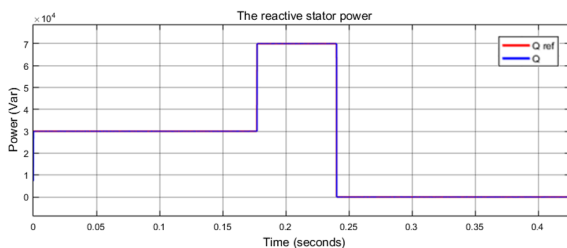


Figure 8. Backstepping control simulation results showing how changes in rotor resistance affect reactive power

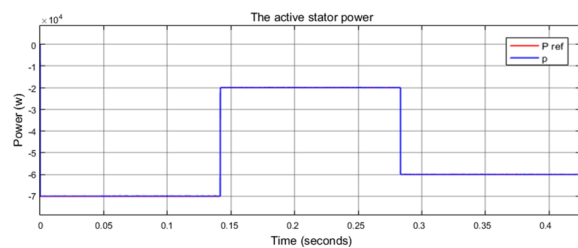


Figure 9. Results of a simulation employing Backstepping control to examine how changes in rotor resistance affect active power

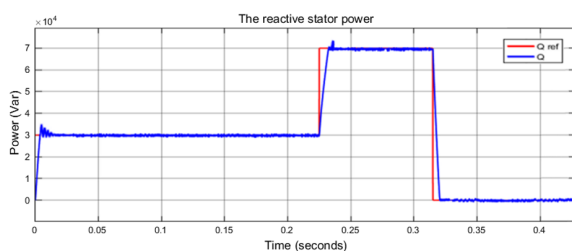


Figure 10. Results of a simulation utilizing FLC control to examine how changes in rotor resistance affect reactive power

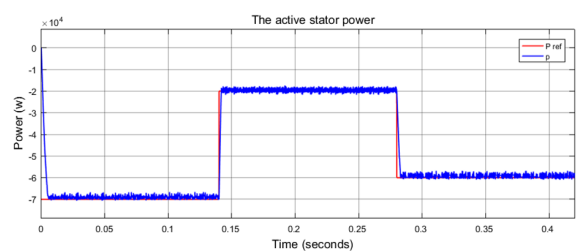


Figure 11. Results of a simulation utilizing FLC control to examine how changes in rotor resistance affect active power

6.4.2. Teste 2: influence of -35% variation in mutual inductance L_m

Figure 12 demonstrates the influence of variations in rotor mutual inductance on reactive power under Backstepping control for the DFIG and Figure 13 illustrates the influence of variations in rotor mutual inductance on active power when employing Backstepping control for the DFIG. Figure 14 illustrates how variations in rotor mutual inductance influence active power when employing FLC for the DFIG, and Figure 15 illustrates how variations in rotor mutual inductance impact active power when utilizing FLC for the DFIG.

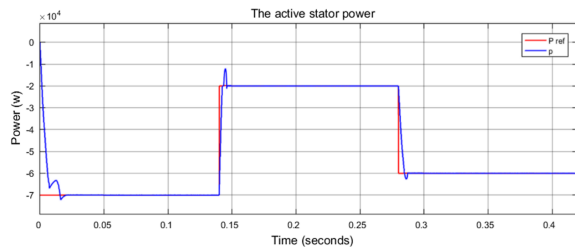


Figure 12. Results of a simulation utilizing Backstepping control to examine how changes in rotor mutual inductance affect reactive power

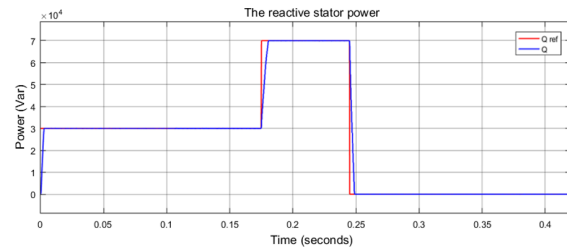


Figure 13. Results of a simulation employing Backstepping control to examine how changes in rotor mutual inductance affect active power

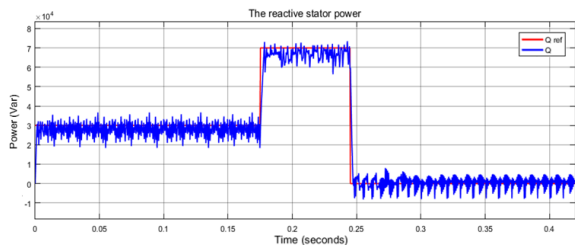


Figure 14. Results of an active power simulation employing FLC control to examine the impact of rotor mutual inductance fluctuations

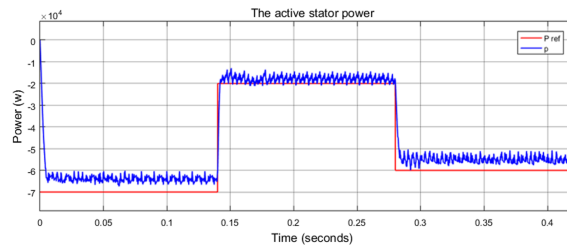


Figure 15. Results of a reactive power simulation employing FLC control for the impact of changes in rotor mutual inductance

7. RESULTS AND DISCUSSION

The outcomes of this study indicate that altering parameters in the DFIG model notably impacts the active and reactive power profiles regulated by FLC, as depicted in Figures 14 and 15. Specifically, increasing the rotor resistance (R_r) by 90% resulted in distinct variations in the FLC control outputs, overshoot (active power, Figure 11), and response times for both active and reactive powers (Figures 10 and 11). Additionally, abrupt oscillations were observed despite an increase in the static error of active and reactive powers by 35% of the nominal value of the mutual inductance (L_m), as illustrated in Figures 14 and 15. This finding suggests that the FLC method is not resistant to internal parametric fluctuations, validating the reliance of the FLC control law on the rotor resistance and mutual inductance of the DFIG. Our results in Figures 8, 9, 12, and 13 show that the Backstepping control also affects the reactive and active power curves under DFIG model parameter changes. However, the robustness and dependability of Backstepping control are demonstrated by its ability to maintain stator active and reactive power tracks relative to their references, even when the rotor resistance R_r rises by 90%. Notably, when the mutual inductance L_m is varied by 35% of its nominal value, there is an increase in reactive power overshoot (Figure 12) and power response time (Figures 12 and 13), with no change in the static error. From these robustness tests, it is evident that variations in resistances and mutual inductances have minimal influence on the performance of Backstepping-based control.

This study investigated the application of the Backstepping control law to the power generation system of a doubly-fed asynchronous generator (DFIG). While earlier studies have explored various control methods for DFIGs, they have not explicitly addressed the comparative influence of Backstepping and fuzzy logic on performance metrics under varying operating conditions. We found that Backstepping control provided superior reference tracking and reduced overshoot compared to FLC under various conditions.

The proposed method in this study tended to have a significantly higher proportion of effective active and reactive power regulation, showing improved dynamic response. Our study suggests that higher robustness against parameter variations in DFIGs is not associated with poor performance in power regulation. The proposed Backstepping method may benefit from systematic design without adversely impacting the adaptability of FLC. However, the FLC's flexibility in handling non-linear systems like wind turbines offers strong performance, despite parameter fluctuations. This study explored a comprehensive control strategy with Backstepping and FLC. However, further and in-depth studies may be needed to confirm their efficacy, especially

regarding their long-term performance under different operational scenarios. Our findings imply that both control methods are effective for enhancing DFIG wind turbine reliability and power quality.

Future research could optimize these controllers further, explore hybrid approaches, and test their adaptability in more complex scenarios, including energy storage integration for broader renewable energy applications. Recent observations suggest that advanced control methods like Backstepping and fuzzy logic significantly improve the stability and performance of DFIG-based wind turbine systems. Our findings provide conclusive evidence that these methods are associated with enhanced power regulation and robustness, not merely due to elevated adaptability to parameter variations, can be seen in Table 2.

Table 2. Comparison between fuzzy logic and Backstepping control

| Control type | Response time (seconds) | Static error |
|----------------------|-------------------------|--------------|
| Fuzzy logic control | 0.0024s | 0.9741 |
| Backstepping control | 0.00031s | 0.996 |

8. CONCLUSION

The numerical simulations clearly show the advantages of Backstepping and FLCs for DFIG-based wind turbine systems. Both methods effectively regulated active and reactive power with good dynamic responses. Backstepping control provided superior reference tracking and reduced overshoot compared to fuzzy logic under various conditions. Fuzzy logic, with its simple, data-driven approach, offered strong performance and robustness for complex nonlinear systems like wind turbines. The comparative analysis revealed that Backstepping control excelled in performance metrics such as overshoot and tracking speed, thanks to its systematic design. In contrast, FLC proved robust against parameter variations due to its flexible rule-based approach. Both techniques are effective for enhancing DFIG wind turbine reliability and power quality. Future research could optimize these controllers further and explore hybrid approaches, as well as test their adaptability in more complex scenarios, including energy storage integration for broader renewable energy applications.

APPENDIX 1: DFIG PARAMETERS

Rated power: 80 kW.

Rotor resistance = 0.019 Ω .

Stator resistance $R_s = 0.018 \Omega$.

Mutual inductance $M = 8.17 \text{ mH}$.

Stator inductance $L_s = 8.49 \text{ mH}$.

Rotor inductance $L_r = 2.587 \text{ mH}$.

Number of pole pairs $p = 3$.

Moment of inertia $J = 1000 \text{ Kg.m}^2$.

Coefficient of friction $f = 0.0024 \text{ N.m.s/r}$.

APPENDIX 2: WIND TURBINE PARAMETERS

Rated power: $P_n = 80 \text{ kW}$.

Radius of the blade $R = 8.3 \text{ m}$.

Number of blades 3.

Gear ratio $G = 80$.

Viscous friction coefficient $f_r = 0.0024 \text{ N.m}^{-1}$

Nominal wind speed $v = 12 \text{ m/s}$.

Moment of inertia $J = 1300 \text{ Kg.m}^2$.





REFERENCES

- [1] S. Jones, L. Anderson, and M. Reed, "Simulation and analysis of complex dynamic systems," *International Journal of Control Systems*, vol. 45, no. 3, pp. 123–136, 2018.
- [2] P. Smith, T. Johnson, and R. Lee, "Advanced simulation techniques for power systems," *IEEE Transactions on Power Systems*, vol. 35, no. 4, pp. 451–463, 2020.
- [3] K. Idjdarene, D. Rekioua, T. Rekioua, and A. Tounzi, "Vector control of autonomous induction generator taking saturation effect into account," *Energy Conversion and Management*, vol. 49, no. 10, pp. 2609–2617, Oct. 2008, doi: 10.1016/j.enconman.2008.05.014.
- [4] R. Vinayakumar, M. Alazab, K. P. Soman, P. Poornachandran, A. Al-Nemrat, and S. Venkatraman, "Deep learning approach for intelligent intrusion detection system," *IEEE Access*, vol. 7, pp. 41525–41550, 2019, doi: 10.1109/ACCESS.2019.2895334.
- [5] G. Dreyfus, J. Martinez, M. Samuelides, M. B. Gordon, F. Badran, and S. Thiria, "Reseaux de Neurones: Methodologie et Applications," *Editions Eyrolles*, 2002.
- [6] S. S. K. V. and D. Thukaram, "Accurate modeling of doubly fed induction generator based wind farms in load flow analysis," *Electric Power Systems Research*, vol. 155, pp. 363–371, Feb. 2018, doi: 10.1016/j.epsr.2017.09.011.
- [7] M. Chen, Z. Gao, and J. Wu, "Control algorithms for generators: a theoretical review," *IEEE Transactions on Energy Conversion*, vol. 34, no. 2, pp. 765–774, 2019.
- [8] H. Wang, Q. Liu, and Y. Chen, "Fuzzy logic control in dynamic systems," *Journal of Control Engineering*, vol. 78, no. 5, pp. 321–333, 2021.
- [9] M. Abouyaakoub and H. Hiji, "Analysis and comparison of mathematical models PV array configurations (series, parallel, series-parallel, bridge-link and total-cross-tied) under various partial shading conditions," in *Lecture Notes in Networks and Systems*, vol. 669 LNNS, 2023, pp. 672–683.




- [10] M. Bendaoud, S. Ladide, and H. Hihi, "Passivity based control of dc-dc converters operating in discontinuous conduction mode," *Journal of Electrical Systems & Automation*, 2022.
- [11] S. Ladide, H. Hihi, and K. Faitah, "Optimal tracking, modeling and control of aerogenerator based on PMSG driven by wind turbine," in *2016 IEEE International Conference on Renewable Energy Research and Applications, ICRERA 2016*, 2016, pp. 891–896, doi: 10.1109/ICRERA.2016.7884464.
- [12] H. Hihi and A. Rahmani, "A Sufficient and necessary conditions for the controllability of switching linear systems," in *2007 IEEE International Conference on Systems, Man and Cybernetics*, Oct. 2007, pp. 3984–3989, doi: 10.1109/ICSMC.2007.4414248.
- [13] W. Soulouh, H. Hihi, and K. Faitah, "Modeling and controlling of a wind turbine generator based on the permanent magnet synchronous machine," in *2014 International Renewable and Sustainable Energy Conference (IRSEC)*, Oct. 2014, pp. 340–345, doi: 10.1109/IRSEC.2014.7059807.
- [14] Y. Moumani, A. J. Laafou, and A. A. Madi, "A comparative study based on proportional integral and backstepping controllers for doubly fed induction generator used in wind energy conversion system," *Archives of Electrical Engineering*, vol. 72, no. 1, pp. 211–228, Jan. 2023, doi: 10.24425/aee.2023.143698.
- [15] M. Nadour, A. Essadki, M. Fdaili, and T. Nasser, "Advanced backstepping control of a wind energy conversion system using a doubly-fed induction generator," in *Proceedings of 2017 International Renewable and Sustainable Energy Conference, IRSEC 2017*, Dec. 2018, pp. 1–6, doi: 10.1109/IRSEC.2017.8477276.
- [16] M. Chahboun and H. Hihi, "Robust control of a wind power system based on a doubly-fed induction generator using a fuzzy controller," in *Lecture Notes in Networks and Systems*, vol. 668 LNNS, 2023, pp. 724–734.
- [17] Y. Djeriri and Z. Boudjema, "Commande robuste par la logique floue et les reseaux de neurones artificiels de la GADA: etude comparative," *Journal of Renewable Energies*, vol. 20, no. 1, pp. 147–160, Oct. 2023, doi: 10.54966/jreen.v20i1.616.
- [18] M. Chahboun and H. Hihi, "A Comparative study between direct and indirect power control of DFIG within wind power system by the stator flux orientation technique," in *2022 IEEE 3rd International Conference on Electronics, Control, Optimization and Computer Science, ICECOCS 2022*, Dec. 2022, pp. 1–6, doi: 10.1109/ICECOCS55148.2022.9983007.
- [19] N. Hamrouni, M. Jraidi, A. Cherif, and A. Dhoubi, "Measurements and simulation of a PV pumping systems parameters using MPPT and PWM control strategies," in *Proceedings of the Mediterranean Electrotechnical Conference - MELECON, 2006*, vol. 2006, pp. 885–888, doi: 10.1109/melcon.2006.1653240.
- [20] M. Bendaoud, S. Ladide, A. El Fathi, H. Hihi, and K. Faitah, "Fuzzy-logic peak current control strategy for extracting maximum power of small wind power generators," *International Transactions on Electrical Energy Systems*, vol. 29, no. 2, p. e2730, Feb. 2019, doi: 10.1002/etep.2730.
- [21] A. Davigny, "Participation aux services système de fermes d' ' eoliennes ' a vitesse variable int ' egrant du stockage inertiel d' ' energie," *These pr ' esent ' ee pour l'obtention du dipl ' ome de Doctorat ^, Ecole Doctorale Sciences Pour l'Ingenieur*, 2007.
- [22] A. Ait Ali, Y. Ouhassan, M. Abouyaakoub, M. Chahboun, and H. Hihi, "The impact of desert regions on solar energy production with the evaluation of groundwater for maintenance: a case study in Morocco," *Sustainability*, vol. 16, no. 13, p. 5476, Jun. 2024, doi: 10.3390/su16135476.
- [23] Y. Zhang, X. Li, and W. Zhao, "Backstepping control for nonlinear power systems," *Journal of Electrical Engineering*, vol. 65, no. 2, pp. 89–97, 2018.
- [24] V. Gupta, "MATLAB/Simulink for power system studies: a comprehensive approach," *Springer*, 2019.
- [25] A. Bangura, M. Errouha, H. Hihi, and Z. Chalh, "Modelling and simulation of the hybrid system PV -wind," *Statistics, Optimization and Information Computing*, 2023.
- [26] H. Hihi, "Contribution a la mod ' elisation et ' a l'analyse des syst ' emes dynamiques hybrides," *Ecole Centrale de Lille*, 2008.
- [27] S. Junco, A. Donaire, A. Rahmani, and H. Hihi, "On the stability of a class of switched bond graphs," in *Proceedings - 22nd European Conference on Modelling and Simulation, ECMS 2008*, Jun. 2008, pp. 478–484, doi: 10.7148/2008-0478.
- [28] H. El Fadil and W. Zhang, *Automatic Control and Emerging Technologies*, vol. 1141. Singapore: Springer Nature Singapore, 2024.
- [29] L. Huang, "Evaluation of control system stability under parametric variations," *Journal of Electrical Engineering Studies*.
- [30] X. Li, H. Sun, and Z. Wang, "Parametric studies and control strategies in power systems," *Control Systems Technology Journal*, vol. 22, no. 4, pp. 401–416, 2021.

BIOGRAPHIES OF AUTHORS






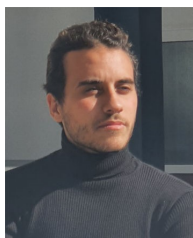
Mbarek Chahboun     obtained his master's degree in Electronic and Embedded Systems from Université Moulay Ismail, Morocco, in 2020. Currently, he is pursuing his Ph.D. in Electrical and Power Engineering at the Systems and Applications Engineering Laboratory, National School of Applied Sciences, Fez, at Sidi Mohamed Ben Abdellah University, Morocco. His research interests include adaptive control, nonlinear control, with applications to power conversion and renewable energy systems, while sharing his expertise through his articles. He can be contacted at email: mbarek.chahboun@usmba.ac.ma.






Mohcine Abouyaakoub    holds a state engineer diploma and an aggregation in electrical engineering. With ten years of combined experience in industry and teaching, he seamlessly integrates his professional background into his pedagogical activities. Currently an professor teaching in preparatory classes for Bac+2 students, and a doctoral candidate at the National School of Applied Sciences in Fes, affiliated with Sidi Mohamed Ben Abdellah University, his research focuses on renewable energies, including studies on solar panels, wind energy, and energy storage systems, while sharing his expertise through his articles. He can be contacted at email: mohcine.abouyaakoub@usmba.ac.ma.






Ali Ait Ali    was born in Rissani Errachidia, Morocco. I work at the National agency for land conservation, surveying, and cartography. He received the master degree in energy in 2022, from National School of Arts and Crafts university Mohammed V. Rabat, He has over eight years of experience in the fields of cartography and energy. I have participated in research days and national and international conferences. Currently, he is preparing a Ph.D. degree at renewable energies at the Laboratory of Engineering, Systems and Applications (LISA) in Sidi Mohamed Ben Abdellah University of Fez, Morocco. Her research is in renewable energy, energy efficiency, material, energy storage, electrical engineering, and thermal energy. He can be contacted at email: ali.aitali@usmba.ac.ma.






Aziz El Mrabet    received the engineering degree in Mechanical Engineering and Automated Systems from Université Sidi Mohamed Ben Abdellah, Ecole Nationale des Sciences Appliquées de Fès, in 2022. He is actively pursuing a Ph.D. in the laboratory of engineering, systems, and applications at the National School of Applied Sciences, Sidi Mohamed Ben Abdellah University, Fez, Morocco. His research focuses on the optimization of a hybrid vehicle. He can be contacted at email: aziz.elmrabet@usmba.ac.ma.






Hicham Hihi    born in Fez, Morocco, he is a full professor at the National School of Applied Sciences and the Laboratory of Engineering, Systems, and Applications (LISA) at Sidi Mohamed ben Abdellah University, Fez. He earned his Ph.D. in Control Engineering from École Centrale Lille, France, in 2008, and his HDR from Cadi Ayyad University, Marrakech, in 2016. He directed Electrical Engineering at ENSA Marrakech (2015-2018) and has chaired the International Conference on Monitoring Industrial Systems since 2011. He was president of the Association of Research and Industrial Innovation (Rinnovaindus) (2015-2019) and has been vice-president since 2019. His research focuses on modeling and simulation of physical systems, energy management of electrical systems and vehicles, and mechatronics. He has over 100 scientific publications and, since 2020, leads the "Renewable Energy and Control Systems" research team. He has been deputy director of LISA at ENSA Fez since 2023 and is involved in various projects. He can be contacted at email: hicham.hihi@usmba.ac.ma.



Hassan Ouabi    he earned his master's degree in Electronics and Embedded Systems from the Faculty of Science and Technology (FST) in Errachidia, Morocco, in 2020. He is currently pursuing a Ph.D. in controlling and optimizing energy in hybrid systems at Hassan II University of Casablanca, Morocco. His research focuses on nonlinear control, energy optimization and management, and observer design, particularly in power systems, renewable energy conversion systems, and hydrogen technology. He can be contacted at email: ouabihassan829@gmail.com.



Youssef El Bid    born in Laayoune, Morocco, he is currently pursuing a Ph.D. this Ph.D. focuses on materials and renewable energy at the Research Team on Energy and Sustainable Development, Higher School of Technology of Guelmim, Ibn Zohr University Agadir, Morocco. He holds a master's degree in Engineering of Concentrated Solar Power Plants, obtained in 2020 from the Faculty of Sciences Semlalia Marrakech, and a professional bachelor's degree in Renewable Energy and Procedures obtained in 2018 from the Higher School of Technology of Guelmim. He can be contacted at email: youssef.elbid@edu.uiz.ac.ma.